

Measurement of the $\chi^{(2)}$ tensor of $\text{GdCa}_4\text{O}(\text{BO}_3)_3$ and $\text{YCa}_4\text{O}(\text{BO}_3)_3$ crystals

Michael V. Pack, Darrell J. Armstrong, and Arlee V. Smith

Department 1112 Lasers, Optics and Remote Sensing, Sandia National Laboratories, Albuquerque, New Mexico 87185-1423

Gerard Aka

Laboratoire de Chimie Appliquée de l'Etat Solide, Ecole Nationale Supérieure de Chimie de Paris, Unité Mixte de Recherche 7574, Centre National de la Recherche Scientifique, 11, Rue P. et M. Curie, 75231 Paris Cedex 05, France

Bernard Ferrand and Denis Pelenc

Laboratoire d'Electronique de Technologie de l'Information, Commissariat à l'Energie Atomique, Technologie Avancées DOPT/STCO DOPT/SCMDO CENG, 17, Rue des Martyrs, 38054 Grenoble Cedex 09, France

Received February 26, 2004; revised manuscript received July 22, 2004; accepted August 24, 2004

Using the separated-beam method, we have measured the full second-order nonlinear optical tensors of the crystals $\text{GdCa}_4\text{O}(\text{BO}_3)_3$ and $\text{YCa}_4\text{O}(\text{BO}_3)_3$. Our d tensors ($d = \chi^{(2)}/2$) differ from those of previous reports but give nearly the same values of d_{eff} for type-I doubling of 1064-nm light. However, for other wavelengths or for type-II doubling, our tensors give values for d_{eff} distinctly different from the alternative tensors.

© 2005 Optical Society of America
OCIS codes: 160.4330, 190.4400.

1. INTRODUCTION

The recently developed nonlinear optical crystals $\text{GdCa}_4\text{O}(\text{BO}_3)_3$ (GCOB) and $\text{YCa}_4\text{O}(\text{BO}_3)_3$ (YCOB) feature easy crystal growth of both pure and rare-earth-doped crystals, high optical transparency, and moderately high nonlinearity. A number of papers have described the linear and nonlinear optical properties of these crystals, including the presentation of several Sellmeier equations that parameterize the refractive indices,¹⁻⁷ and both d_{eff} for various propagation directions and complete or partial d tensors, measured by frequency-doubling 1064-nm light.⁵⁻¹¹ The d tensors were also calculated with molecular orbital theory.^{11,12} In this paper we report new measurements of the refractive indices n_x , n_y , and n_z at 1064 and 532 nm, as well as measurements of the complete d tensors for both GCOB and YCOB.

Both GCOB and YCOB belong to the crystal-symmetry point group m , meaning the unit cell is a right prism in which one crystallographic axis, labeled b by convention, is normal to the mirror symmetry plane containing the other two axes, a and c . This symmetry implies that the principal optical frame $[x, y, z]$, in which the dielectric tensor is diagonal, has one of its axes aligned parallel to b . Further, class- m symmetry allows the three dielectric tensor elements to be unequal, meaning crystals of this class are biaxial. For both YCOB and GCOB, it happens to be the y axis that is aligned with b , where we adhere to the convention $n_x < n_y < n_z$. Additional conventions for class- m crystals are that the angle between the a and c axes is greater than 90° and that $c < a$. For GCOB,

$(a, b, c) = (0.808, 1.598, 0.355)$ nm, whereas, for YCOB, $(a, b, c) = (0.805, 1.590, 0.352)$ nm. The measured angle between the a and the c axes is 101.2° for YCOB² and 101.3° for GCOB.⁷

The orientation of the x and z axes relative to the a and c axes is not fixed by class- m crystal symmetry and can change with wavelength, temperature, and other external influences. However, we observed no change in the orientation for either crystal between the two wavelengths involved in our measurements, 1064 and 532 nm. This is supported by the measurements of Segonds *et al.*² who found no change in orientation over the wavelength range $400 \text{ nm} < \lambda < 2400 \text{ nm}$ in YCOB. Umemura *et al.*¹³ do report a small, wavelength-dependent change with temperature for YCOB, but it is only a few microradians per degree Kelvin, too small to affect our measurements or to be of practical significance in wavelength-conversion applications. The measured angles between the a and c crystallographic axes and the x and z optical frame are $\angle_{az} = 24.7^\circ$ and $\angle_{cx} = 13.5^\circ$ for YCOB² and $\angle_{az} = 26^\circ$, $\angle_{cx} = 15^\circ$ for GCOB.⁷ The relative orientations of the crystallographic frames $[a, b, c]$ and the principal optical frames $[x, y, z]$ are diagrammed in Fig. 1.

The d tensors characterizing the second-order nonlinearity of GCOB and YCOB have the form shown in Fig. 2. This form is implied by crystal symmetry and applies to all class- m crystals in which the y axis is parallel to b . The d tensor has ten independent elements. If we impose Kleinman symmetry, which asserts near equality for elements with permuted subscripts, there are six inde-

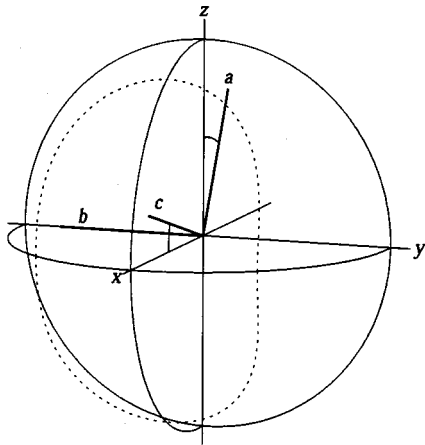


Fig. 1. Diagram of relation between the crystallographic axis system a , b , c and the optical principal axis system x , y , z . The dashed curve shows the loci of phase-matching angles for type-I doubling of 1064-nm light in YCOB. For clarity only the $x > 0$ hemisphere of propagation directions is shown. The mirror image of the dashed curve in the yz plane forms the set of phase-matching directions in the $x < 0$ hemisphere.

$$\begin{array}{c}
 \begin{array}{c} \text{z cut} \\ \text{y cut} \end{array} \\
 \left(\begin{array}{cccccc}
 d_{xxx} & d_{xyy} & d_{xzz} & 0 & d_{xzx} & 0 \\
 0 & 0 & 0 & d_{yyz} & 0 & d_{yxy} \\
 d_{zxx} & d_{zyy} & d_{zzz} & 0 & d_{zxx} & 0
 \end{array} \right) \\
 \begin{array}{c} \text{x cut} \\ \text{y cut} \end{array}
 \end{array}$$

Fig. 2. Form of the d tensor for YCOB and GCOB. The solid lines connect elements that are measured with various crystal cuts, as labeled. The dashed lines connect elements that are equal under Kleinman symmetry.

pendent elements. Most recent measurements of the d tensor measured only a few of the elements on the basis of Maker fringe methods or measuring d_{eff} along a few phase-matching directions. Only Wang *et al.*¹⁰ attempted to evaluate all six elements for both crystals. Their derivation of d was based on adjusting the individual tensor elements to fit measured values of d_{eff} for type-I doubling 1064-nm light over a range of phase-matching angles. In contrast to this indirect deduction of d , we have directly and independently measured all ten of the coefficients for both YCOB and GCOB by using the separated-beams method.^{14–16} We will compare our measured d tensor with other reported values, and we will use it to compute d_{eff} along various phase-matching directions for comparison with measurements reported in the literature.

When the orientation of the optical frame is wavelength independent, as it is for GCOB and YCOB, the loci of phase-matching angles form symmetric loops around each of the twin optic axes, which lie in the xz plane or around one of the principal axes, x , y , or z . In Fig. 1 we show as a dashed curve the loci of phase-matching directions for type-I frequency doubling of 1064-nm light in YCOB. It loops around the x axis and is symmetric on reflection in any of the principal planes. For the sake of

clarity, we do not show the companion loop around the $-x$ axis because it corresponds to reversal of the direction of propagation of all three waves, which affects neither the refractive indices, and thus the phase-matching angles, nor the magnitude of d_{eff} . The symmetry on reflection in the a - c plane inherent to class- m crystals means the nonlinear coefficient is unchanged on reflection of the propagation vector in the a - c plane. That is, if $k_y \rightarrow -k_y$, d_{eff} is unchanged, so we need concern ourselves with only the right-hand half of the phase-matching loop, where $k_y > 0$. The lack of crystal symmetry between the upper ($k_z > 0$) and the lower ($k_z < 0$) right-hand octants means that d_{eff} is not symmetric in the two octants, implying that complete characterization of d_{eff} requires that we specify it in both octants. One of these octants is adjacent to either the positive or the negative a axis, and the other is adjacent to either the positive or the negative c axis. We refer to these octants as the a or c octant. Similar arguments apply to phase-matching loops for other mixing processes that encircle the optic axes or the y or z axes. In each case, a octants and c octants have different nonlinearities. This means that in calculating d_{eff} it is essential that the propagation direction relative to the $[a, b, c]$ frame be known. We will see that this requirement also applies to our measurements based on the separated-beams method.

2. CRYSTAL GROWTH

The YCOB and GCOB crystals were grown by Czochralski pulling with a $\langle 010 \rangle$ -oriented seed in a 100-mm diameter, 100-mm-high iridium crucible. Flowing nitrogen provided a neutral atmosphere. GCOB has perfect congruent melting behavior so Czochralski pulling is a suitable growth method, but YCOB has a miscibility gap in the liquid phase according to Klimm *et al.*¹⁷ Nevertheless, if the cooling rate is sufficiently slow, with adequate mixing of the melt, the Czochralski method yields pure YCOB. Typical pulling and rotation rates were 1 mm/h and 25 rpm for GCOB and 3 mm/h and 25 rpm for YCOB. Typical crystal sizes were 50 mm in diameter and 60–120 mm in length. Postgrowth annealing under atmosphere at 1250 °C for 24 h eliminated internal stress, resulting in crack-free crystals of good optical quality.

3. MEASUREMENT METHOD

We described the separated-beams method in earlier papers.^{14–16} It permits straightforward measurement of the entire nonlinear tensor, including the relative signs of the coefficients. Briefly, we use three samples of both YCOB and GCOB cut for propagation along the three principal axes, x , y , and z . The input face is normal to the principal axis, but the output face is tilted approximately 30° from normal with the tilt lying in one of the principal planes. When a single fundamental beam is incident on the input face, as many as five second-harmonic beams emerge, angularly separated by the prism effect of the tilted exit face. We measure two of them, known as the free waves, which are polarized along the two eigenpolarization directions. For example, in the y -cut sample the two free waves are polarized parallel to the x and z

axes. The strength of each free wave varies with the polarization angle of the linearly polarized fundamental beam. In the case of GCOB and YCOB the x -polarized free wave has interfering contributions from d_{xxx} , d_{xzz} , and d_{xxz} , as indicated in Fig. 2 by the lines labeled y cut that connect these elements. The d_{xxx} term contributes with a strength proportional to the square of the x component of the fundamental electric field, the d_{xzz} contribution is proportional to the square of the z component of the fundamental field, and the d_{xxz} contribution is proportional to the product of the x and z components of the fundamental field. By measurement of the strength of the x -polarized second-harmonic free wave as the polarization angle of the fundamental polarization is rotated through 180° , the strengths of the three contributions can be individually determined, including their relative signs. Note that if only the optical frame is used to orient the sample without knowledge of the crystallographic frame the sign of the d_{xxz} contribution is ambiguous. One can remove this ambiguity by locating the a axis and noting whether this term contributes constructively or destructively when the fundamental field is polarized along the a axis. This satisfies the requirement stated earlier that the polarization directions must be related to the crystallographic axes for the relative signs of the coefficients to be meaningful.

From Fig. 2 it is apparent that by using both the y -cut and the z -cut samples we can find the relative values of each element of the first row of d , including their relative signs. Similarly, using both the y -cut and the x -cut samples, we can find the relative values of each element of the last row. The values of the two coefficients on the second row can be individually measured with the x -cut (d_{yyz}) and z -cut (d_{yxy}) samples. The dashed lines in the figure connect pairs of elements that are equal under Kleinman symmetry, and it is a safe assumption that both members of each pair have the same sign. This allows us to connect the signs of all elements. Note that elements d_{xxx} and d_{zzz} are measured twice. This redundancy, along with comparisons of elements that are nearly equal by Kleinman symmetry, means that each element is measured twice, providing a check on the measurement quality. Our d_{ijk} values are put on an absolute scale by comparison with the d_{zxy} element of the KDP crystal, which has a consensus value¹⁸ of 0.39 pm/V.

The strength of the contribution to a free wave from each tensor element is proportional to constants that we call \mathcal{N}_{ijk} . These can be computed from the refractive in-

dices of the fundamental and harmonic waves plus the exit face angle. Most importantly, these terms are proportional to the inverse of the phase-velocity mismatch, $\Delta k = k_{2\omega} - k_{\omega_1} - k_{\omega_2}$, which is proportional to the small difference between refractive indices and which is a major contributor to the measurement uncertainty. We measure the refractive indices by measuring the refraction angles of the (up to) five second-harmonic beams. Our results are listed in Table 1. Among the numerous Sellmeier equations in the literature for these crystals, we find the best agreement with that published by Aka *et al.*,⁷ whose values are also listed in the table. On the basis of the precision with which we can measure the exit face angles and the beam refraction angles, we expect the uncertainties in the indices to be approximately ± 0.0003 , and this is verified by comparison of the twin measurements of each index from two different crystal samples.

4. GCOB MEASUREMENT

A. y -Cut Crystal

This crystal sample is cut for propagation along the y axis. The input face is normal to the y axis, and the exit face is tilted by 29.941° in the xy plane. This sample generates two second-harmonic free waves, one x polarized and the other z polarized. The x -polarized free wave has contributions from tensor elements d_{xxx} , d_{xzz} , and d_{xxz} , and the energy of this free wave depends on the polarization angle of the fundamental ψ according to

$$\mathcal{F}_x = CU_1^2 |d_{xxx}\mathcal{N}_{xxx} \cos^2(\psi) + d_{xzz}\mathcal{N}_{xzz} \sin^2(\psi) + d_{xxz}\mathcal{N}_{xxz} \sin(2\psi)|^2, \quad (1)$$

where the \mathcal{N} 's are constants that depend on the refractive indices and the exit face angle, U_1 is the fundamental pulse energy, and C is a constant, common to all of our measurements, that depends on the pulse duration and beam diameter of the input fundamental light. Similarly, the z -polarized free wave is given by

$$\mathcal{F}_z = CU_1^2 |d_{zxx}\mathcal{N}_{zxx} \cos^2(\psi) + d_{zzz}\mathcal{N}_{zzz} \sin^2(\psi) + d_{zxz}\mathcal{N}_{zxz} \sin(2\psi)|^2. \quad (2)$$

These measurements are calibrated against the z -polarized free wave from the reference KDP crystal that is cut for propagation along $x = y$. The z -polarized free-wave energy for KDP is

$$\mathcal{F}_z = CU_1^2 |d_{zxy}\mathcal{N}_{zxy} \cos^2(\psi)|^2, \quad (3)$$

Table 1. Measured Refractive Indices of YCOB and GCOB

Crystal Sample	n_x (1064 nm)	n_x (532 nm)	n_y (1064 nm)	n_y (532 nm)	n_z (1064 nm)	n_z (532 nm)
GCOB (x cut)			1.7055	1.7277	1.7143	1.7367
GCOB (y cut)	1.6810	1.7015			1.7145	1.7369
GCOB (z cut)	1.6812	1.7015	1.7059	1.7276		
Sellmeier ⁷	1.6806	1.7010	1.7048	1.7272	1.7138	1.7362
YCOB (x cut)			1.6975	1.7192	1.7081	1.7302
YCOB (y cut)	1.6670	1.6864			1.7081	1.7302
YCOB (z cut)	1.6673	1.6867	1.6980	1.7196		
Sellmeier ⁷	1.6669	1.6861	1.6979	1.7191	1.7080	1.7299

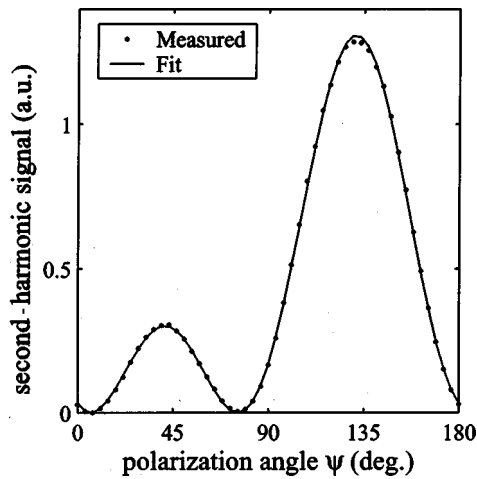


Fig. 3. Pulse energy of x -polarized second-harmonic free wave versus polarization angle of the fundamental for the y -cut GCOB sample. The quarter-wave plate is removed so that the fundamental light is polarized linearly at the crystal. The polarization angle ψ is measured from the positive x axis toward the positive z axis.

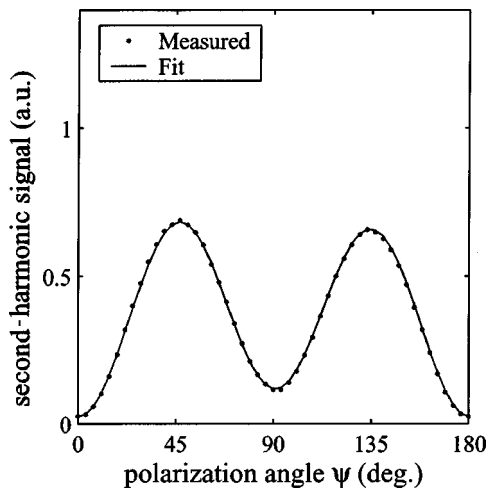


Fig. 4. Pulse energy of x -polarized second-harmonic free wave versus polarization angle of the fundamental light incident on the quarter-wave plate for the y -cut GCOB sample.

and we use the standard value of 0.39 pm/V for d_{zxy} .

To extract the values of the individual d_{ijk} values for GCOB, we measure the free-wave energy as the polarization angle of the linearly polarized fundamental light is rotated through 180° by use of a half-wave plate. A curve of free-wave energies is shown in Fig. 3. We fit these data with a function of the form

$$\mathcal{F}_x = |A \cos^2(\psi + \epsilon) + B \sin^2(\psi + \epsilon) + C \sin(2\psi + 2\epsilon)|^2. \quad (4)$$

The ϵ is included to account for a small offset of ψ relative to the x and z directions. Unfortunately, for this particular functional form the fit parameters A , B , C , and ϵ are ambiguous. There is no unique value of ϵ that gives the best fit. We could resolve this by measuring ϵ directly, but, instead, we chose to insert a quarter-wave plate just before the crystal with its fast and slow axes aligned along the crystal sample's x and z axes. For a wave plate with exactly one-quarter wave retardation, aligned exactly with the crystal axes, the measured free-wave energy would have the form

$$\mathcal{F}_x = |A \cos^2(\psi + \epsilon) - B \sin^2(\psi + \epsilon)|^2 + |C \sin(2\psi + 2\epsilon)|^2, \quad (5)$$

where ψ is the polarization angle of the fundamental light before the quarter-wave plate. In practice, we must allow for imperfect retardation and alignment, in which case the functional form we use is

$$\mathcal{F}_x = |AE_1^2(\psi) + BE_2^2(\psi) + 2CE_1(\psi)E_2(\psi)|^2, \quad (6)$$

where

$$E_1(\psi) = \cos(\gamma)\cos(\psi + \epsilon) - i \exp(i\delta)\sin(\gamma)\sin(\psi + \epsilon), \quad (7)$$

$$E_2(\psi) = \sin(\gamma)\cos(\psi + \epsilon) + i \exp(i\delta)\cos(\gamma)\sin(\psi + \epsilon). \quad (8)$$

The ϵ accounts for a small offset in ψ before the quarter-wave plate, δ accounts for a small error in the quarter-wave plate retardation, and γ accounts for a small misalignment between the quarter-wave plate axes and the crystal axes. The value of δ is consistently approximately 2° , and the values of γ and ϵ are typically less than

Table 2. Measured Values of d_{ijk} Terms for Frequency-Doubling 1064-nm Light^a

Crystal Sample	d_{xxx}	d_{xyy}	d_{yyx}	d_{xzz}	d_{zzx}	d_{xxz}	d_{zxx}	d_{yyz}	d_{zyy}	d_{zzz}
GCOB x cut								1.66 ± 0.043	1.67 ± 0.037	-1.18 ± 0.028
GCOB y cut	0.27 ± 0.022			-0.58 ± 0.018	-0.61 ± 0.024	-0.36 ± 0.023	-0.32 ± 0.017			-1.21 ± 0.028
GCOB z cut	0.29 ± 0.025	0.21 ± 0.035	0.23 ± 0.025							
YCOB x cut								1.62 ± 0.039	1.62 ± 0.036	-1.19 ± 0.035
YCOB y cut					-0.59 ± 0.020		-0.30 ± 0.016			-1.20 ± 0.035
YCOB z cut	0.155 ± 0.012	0.235 ± 0.024	0.24 ± 0.023							

^aIn picometers per volt.

2° but variable from measurement to measurement because of slight misalignments introduced when the crystal and wave plate are removed and replaced. In Fig. 4 we show the measured free-wave energies and a fit by using a function of this form. This measurement returns the magnitudes of A , B , and C , but the sign of C is ambiguous. To determine this sign, we use the measurement described above without the quarter-wave plate.

For a reliable measurement, it is necessary to verify that the input face is normal to the y axis and to locate the a axis. If the input face were tilted slightly in the yz plane, the nominally z -polarized light would contain a small y component, meaning the d_{xyy} coefficient would interfere with the d_{xzz} coefficient in generating the x -polarized free wave. Similarly, the z -polarized free wave would have unwanted contributions from d_{yxy} and d_{zyy} . The quality and consistency of the functional fits to the data provide one check on the crystal alignment. We use x-ray diffraction to provide a second check and to locate the a axis. Our x-ray measurement confirms that the orientation of the input face of the y -cut GCOB sample is normal to the b ($=y$) axis within the 0.5° precision of the measurement and also indicates that the a axis lies in the range $\psi > 90^\circ$ in which we find that the interference of the d_{xxz} term contribution in Eq. (4) is constructive. The results listed in Table 2 on the row labeled GCOB y cut summarize the values of d_{xxx} , d_{xzz} , and d_{xxz} we derived from the x -polarized free wave, plus the values of d_{zxx} , d_{zzz} , and d_{zxx} we derived from the z -polarized free wave. The pairs connected by Kleinman symmetry are d_{xzz} and d_{zxx} , which have independently measured values of -0.58 and -0.61 pm/V, and d_{xxz} and d_{zxx} , which have independently measured values of -0.36 and -0.32 pm/V. If we assume that Kleinman symmetry holds, and there is no reason to doubt it in this case, the consistency of these values support the assigned uncertainties listed in Table 2.

B. x-Cut Crystal

The input face of the x -cut GCOB crystal is normal to the x axis, and the exit face is tilted by 30.037° in the xy plane. There are two free waves polarized along y and z . The y -polarized free-wave energy has the form

$$\mathcal{F}_y = CU_1^2 |d_{yyz} \mathcal{N}_{yyz} \sin(2\psi)|^2, \quad (9)$$

whereas the z -polarized free wave has the form

$$\mathcal{F}_z = CU_1^2 |d_{zzz} \mathcal{N}_{zzz} \sin^2(\psi) + d_{zyy} \mathcal{N}_{zyy} \cos^2(\psi)|^2. \quad (10)$$

The magnitude of d_{yyz} is determined from the y -polarized free wave, but its sign is not, whereas the magnitudes and relative signs of d_{zzz} and d_{zyy} are found from the z -polarized free wave. No quarter-wave plate is needed for this crystal sample because the functional fits to the measured free-wave energies are unambiguous. The values of d_{yyz} and d_{zyy} , which are equal by Kleinman symmetry, have measured values of 1.66 and 1.67 pm/V. It is not necessary to know the precise orientation of the crystallographic axes in analyzing these results. Location of the a axis is not needed, and, because of the relatively large values of the three d coefficients involved compared with those that would interfere in the case of imperfect

alignment, the sensitivity of the results to slight deviations of the input face normal from the x axis is reduced. Nevertheless, we measured the face normal by using x-ray diffraction and found it to be normal to the x axis within the measurement precision of approximately 0.5°.

C. z-Cut Crystal

The input face of this sample is nominally normal to the z axis, and the exit face is tilted by 30.1335° in the xz plane. There are two free waves, an x -polarized wave with the form

$$\mathcal{F}_x = CU_1^2 |d_{xxx} \mathcal{N}_{xxx} \cos^2(\psi) + d_{xyy} \mathcal{N}_{xyy} \sin^2(\psi)|^2 \quad (11)$$

and a y -polarized wave with the form

$$\mathcal{F}_y = CU_1^2 |d_{yyx} \mathcal{N}_{yyx} \sin(2\psi)|^2. \quad (12)$$

Location of the a axis is not needed in deriving these coefficients. The orientation of the input face normal is checked by x-ray diffraction and found to be aligned with the z axis within measurement precision. However, a small tilt in the zx plane will, in effect, mix some of the large d_{zxx} coefficient into the d_{xxx} coefficient without changing the form of the ψ dependence. Similarly, the d_{zyy} coefficient will interfere with the d_{xyy} coefficient. Consequently, the uncertainties we quote for d_{xxx} and d_{xyy} are relatively large compared with those for the other coefficients. Small tilts in the yz plane, on the other hand, are detectable because they would change the form of the angular dependence of the free-wave energy, so we are confident such tilts are negligible.

5. YCOB MEASUREMENT

A. y-Cut Crystal

Our x-ray measurements indicate that the entrance face normal of this sample is parallel to the y axis within measurement limits. The exit face is tilted by 30.1345° in the xy plane. The measurements and analysis for this sample parallel those for the GCOB y -cut sample described above, with the exception that for YCOB the phase mismatch for the d_{xxz} term is small, making it difficult to pick out the relatively small contributions from the d_{xxx} and d_{xzz} terms. For this reason, we do not report measurements based on the x -polarized free wave. However, the z -polarized free wave is analyzed, and its three contributing coefficients are reported. We derive values of d_{zxx} , d_{zxx} , and d_{zzz} for YCOB that are nearly identical to those we measured for GCOB, as may be seen from Table 2.

B. x-Cut Crystal

Our x-ray measurements indicate that the normal to the entrance face of this sample is parallel to the x axis within measurement error. The exit face is tilted by 30.3137° in the xy plane. The measurements and analysis parallel those of the x -cut GCOB crystal, and our measured values of d_{yyz} , d_{zyy} , and d_{zzz} are identical to those we measured for GCOB within our measurement errors.

Table 3. Comparison of Measured d_{ijk} Terms for Frequency-Doubling 1064-nm Light in GCOB^a

Reference	d_{xxx}	d_{xyy}/d_{yyx}	d_{xzz}/d_{zxx}	d_{xxz}/d_{zxx}	d_{yyz}/d_{zyy}	d_{zzz}
This paper	0.28	0.212/0.228	-0.58/-0.61	-0.36/-0.32	1.66/1.67	-1.20
Wang ¹⁰	0	0.27	-0.85	0.2	2.23	-1.87
Aka ⁷	—	0.33	-0.87	—	2.4	—
Adams ⁸	—	0.22 ± 0.05	—	—	1.72 ± 0.13	—
Chen ¹² (GAUSSIAN)	0.04	0.128	-0.17	0.148	0.74	-0.92
Chen ¹² (CNDO)	0.05	0.166	-0.22	0.162	1.0	-1.14

^a In picometers per volt.**Table 4. Comparison of Measured d_{ijk} Terms for Frequency-Doubling 1064-nm Light in YCOB^a**

Reference	d_{xxx}	d_{xyy}/d_{yyx}	d_{xzz}/d_{zxx}	d_{xxz}/d_{zxx}	d_{yyz}/d_{zyy}	d_{zzz}
This paper	0.155	0.235/0.24	-0.59/-0.59	-0.30/-0.30	1.62/1.62	-1.20
Wang ¹⁰	0	0.24	-0.73	0.41	2.35	-1.6
Aka ⁷	—	0.34	-0.71	—	2.03	—
Adams ⁸	—	0.26 ± 0.04	—	—	1.69 ± 0.17	—
Chen ¹¹ (measured)	—	—	—	—	1.36	-0.93
Chen ¹¹ (GAUSSIAN)	-0.104	-0.015	-0.253	0.12	0.757	-1.02
Chen ¹¹ (CNDO)	0.056	0.128	-0.186	0.151	1.081	-1.236

^a In picometers per volt.

C. z-Cut Crystal

This crystal is nominally cut for propagation along the z axis. However, x-ray measurements indicate that the normal to the input face is tilted by 2.5° from the z axis in the yz plane. We confirmed this by positioning the crystal between crossed polarizers such that a white-light beam propagated parallel to the input face along the x axis. The crystal was rotated to find the best extinction, and the resulting angle between the input face and the polarization axis verified the tilt of the input face relative to the principal axes. The angle between the entrance and the exit faces is 30.065° with the tilt lying in the xz plane. We compensated for the miscut entrance face by tilting the crystal slightly so the fundamental beam propagated along the z axis. This should have little effect on the measurement accuracy if the exit angle is adjusted in the calculation of \mathcal{N}_{yyz} . The result is a set of measured d_{xxx} , d_{xyy} , and d_{yyx} values with small uncertainties. Kleinman symmetry implies equality of d_{xyy} and d_{yyx} , and this is confirmed by our measured values. The measurement of d_{xxx} is relatively unaffected by the crystal misalignment because both the fundamental and the harmonic waves are x polarized and the corrective tilt is in the yz plane. The primary effect of misalignment is to slightly change the exit angle, which we take into account in calculating \mathcal{N}_{xxx} . We find $d_{xxx} = 0.155$ pm/V for YCOB compared with a value of 0.28 pm/V for GCOB.

6. COMPARISON WITH OTHER MEASUREMENTS

Tables 3 and 4 compare our d tensors with previously reported values for GCOB and YCOB. We will briefly summarize the methods and results of previous measurements and computations.

A. GCOB

Aka *et al.*⁷ made absolute measurements of d_{eff} by using type-I, phase-matched frequency doubling of a cw 1064-nm laser along two phase-matching directions lying in the xz principal plane. Their measurements do not rely on comparisons with a reference crystal but, instead, carefully characterize the fundamental beam and use accepted theories for second-harmonic generation of focused beams in the presence of walk-off.¹⁹ They report $d_{\text{eff}} = 0.48$ pm/V along the direction ($\theta = 19.7^\circ$, $\phi = 0^\circ$) and $d_{\text{eff}} = 1.1$ pm/V along the direction ($\theta = 19.7^\circ$, $\phi = 180^\circ$), indicating a larger value for the a octant than for the c octant. Type-I mixing in this case implies a y -polarized fundamental beam produces a second-harmonic beam polarized in the xz plane. Using the expression for d_{eff} in the xz plane,

$$d_{\text{eff}} = d_{xyy} \cos(\theta + \rho) \cos \phi - d_{zyy} \sin(\theta + \rho), \quad (13)$$

gives $d_{xyy} = 0.33$ and $d_{zyy} = 2.4$. The same paper reports a similar measurement along the direction ($\theta = 90^\circ$, $\phi = 46^\circ$) by use of a z -polarized fundamental to generate harmonic light polarized in the xy plane. The measured value of $d_{\text{eff}} = 0.63$ pm/V, and the expression for d_{eff} in the xy plane is

$$d_{\text{eff}} = d_{xzz} \sin(\phi + \rho), \quad (14)$$

from which $d_{xzz} = 0.87$ pm/V. These values are consistently approximately 50% larger than ours, but we can offer no explanation for the difference. They also report $d_{\text{eff}} = 0.80$ pm/V along the direction ($\theta = 67^\circ$, $\phi = 46^\circ$) and $d_{\text{eff}} = 1.8$ pm/V along the direction ($\theta = 67^\circ$, $\phi = 134^\circ$). These measurements cannot be used to find individual d_{ijk} values, but they can be compared with values computed from our measured d tensor. They are larger than ours by approximately 35%.

Wang *et al.*¹⁰ measured d_{eff} for phase-matched doubling of 1064-nm light along nine different phase-matching directions. Their measurements are calibrated by comparison with doubling in a KTP crystal. Their d_{eff} values are plotted in Fig. 5. From these nine values of d_{eff} , they deduced the individual tensor elements listed in Table 3. The value for d_{zyy} in their report appears to have its sign reversed in a typographical error so we have corrected it in Table 3. We note that the same coefficient for YCOB has the correct sign in their paper.

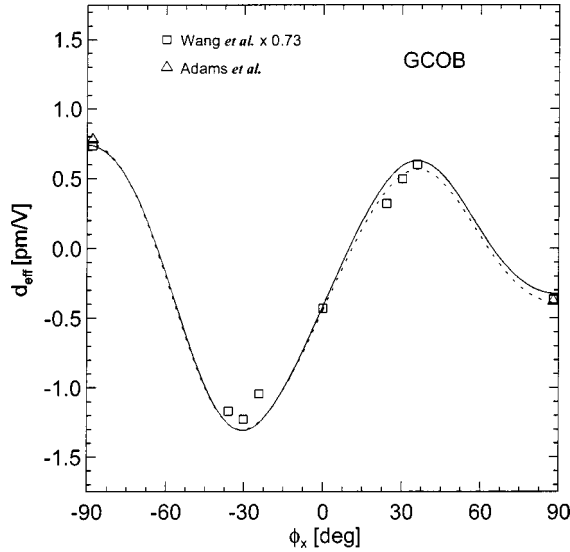


Fig. 5. Calculated values of d_{eff} for type-I frequency doubling of 1064-nm light in GCOB. The solid curve is calculated with our d tensor, and the dashed curve is $0.73 \times d_{\text{eff}}$ computed with Wang's d tensor.¹⁰ Note that we reversed the sign of d_{zyy} in Wang's tensor, as discussed in the text. The symbols indicate the measured values of Adams *et al.*⁸ and the adjusted values of Wang *et al.*¹⁰

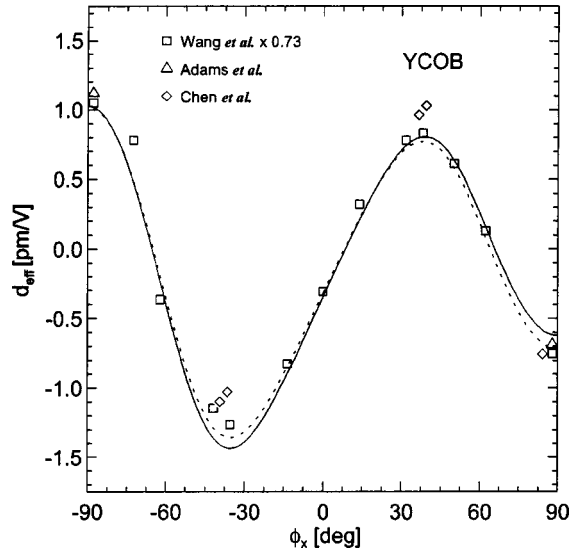


Fig. 6. Calculated values of d_{eff} for type-I frequency doubling of 1064-nm light in YCOB. The solid curve is calculated with use of our d tensor, and the dashed curve is $0.73 \times d_{\text{eff}}$ computed with Wang's d tensor.¹⁰ The symbols indicate the measured values of Adams *et al.*⁸ and the adjusted values from Wang *et al.*¹⁰ and Chen *et al.*¹¹

Adams *et al.*⁸ measured d_{eff} for phase-matched doubling of 1064-nm light in GCOB with calibration against similar measurements in KTP. They find $d_{\text{eff}} = 0.78$ pm/V along $(\theta = 20^\circ, \phi = 0^\circ)$ and 0.38 pm/V along $(\theta = 160^\circ, \phi = 0^\circ)$. Evidently the orientation of their optical axis system relative to the crystallographic axis system is different from the customary one because d_{eff} is larger for $(\theta = 20^\circ, \phi = 0^\circ)$ than for $(\theta = 160^\circ, \phi = 0^\circ)$. Despite this difference, it is still possible to find the relative magnitudes of d_{xxy} and d_{zyy} from their information. It indicates $|d_{xxy}| = 0.22 \pm 0.05$ pm/V and $|d_{zyy}| = 1.72 \pm 0.13$ pm/V. These are in good agreement with our values.

Chen *et al.*¹² used two molecular orbital calculation programs, CNDO and GAUSSIAN 92, to compute the coefficients listed in Table 3. Overall, their results correlate reasonably with ours, but the discrepancy for individual elements is quite large.

B. YCOB

Aka *et al.*⁷ measured d_{eff} values along four type-I phase-matching directions for doubling 1064-nm light. They reported $d_{\text{eff}} = 0.78$ pm/V for $(\theta = 31.7^\circ, \phi = 0^\circ)$, $d_{\text{eff}} = 1.35$ pm/V for $(\theta = 31.7^\circ, \phi = 180^\circ)$, $d_{\text{eff}} = 0.39$ pm/V for $(\theta = 90^\circ, \phi = 35.3^\circ)$, and $d_{\text{eff}} = 1.82$ pm/V for $(\theta = 114^\circ, \phi = 145^\circ)$. From that information they deduced $d_{xzz} = -0.71$ pm/V, $d_{xxy} = 0.34$ pm/V, and $d_{zyy} = 2.03$ pm/V. Like their GCOB results, these d_{ijk} values are significantly larger than ours.

Adams *et al.*⁸ measured d_{eff} for type-I frequency doubling of 1064-nm light in the xy principal plane of YCOB by using KTP as the calibration reference. They found $d_{\text{eff}} = 1.12$ pm/V along $(\theta = 33^\circ, \phi = 0^\circ)$ and $d_{\text{eff}} = 0.69$ pm/V along $(\theta = 147^\circ, \phi = 0^\circ)$. As noted for GCOB, their optical axis system is oriented relative to the crystallographic system in a nonstandard way, but we can say that their values imply $|d_{xxy}| = 0.26 \pm 0.04$ pm/V and $|d_{zyy}| = 1.69 \pm 0.17$ pm/V. They concluded that YCOB, GCOB, and LCOB have identical d_{xxy} coefficients and identical d_{zyy} coefficients within their measurement error.

Chen *et al.*¹¹ used a Maker fringe method for second-harmonic generation of 1064-nm light to measure $d_{xxx} \approx 0.0$ pm/V, $d_{zzz} = \pm 0.93$ pm/V, $d_{zyy} = \pm 1.36$ pm/V, $d_{xxy} \approx 0.0$ pm/V, $d_{xzz} \ll 1$ pm/V, and $d_{zxx} \ll 1$ pm/V. They calibrated their measurements against LiB_3O_5 . The same paper reports measurements of d_{eff} along various phase-matching directions, calibrated against KTP nonlinearity. We have adjusted their values by using improved values for d_{eff} of KTP²⁰ to give $d_{\text{eff}} = 0.77$ pm/V along $(\theta = 32^\circ, \phi = 0^\circ)$, $d_{\text{eff}} = 0.76$ pm/V along $(\theta = 32^\circ, \phi = 9^\circ)$, $d_{\text{eff}} = 1.03$ pm/V along $(\theta = 64.5^\circ, \phi = 35.5^\circ)$, $d_{\text{eff}} = 0.96$ pm/V along $(\theta = 66.8^\circ, \phi = 35.4^\circ)$, $d_{\text{eff}} = 1.03$ pm/V along $(\theta = 113.2^\circ, \phi = 35.4^\circ)$, and $d_{\text{eff}} = 1.10$ pm/V along $(\theta = 115.5^\circ, \phi = 35.5^\circ)$. They also used the molecular orbital models CNDO and GAUSSIAN to compute the full d tensor.

Wang *et al.*¹⁰ measured d_{eff} along 13 phase-matching directions for type-I frequency doubling of 1064-nm light. Their data are plotted in Fig. 6. On the basis of these values, they deduced the values for the individual tensor coefficients listed in Table 4.

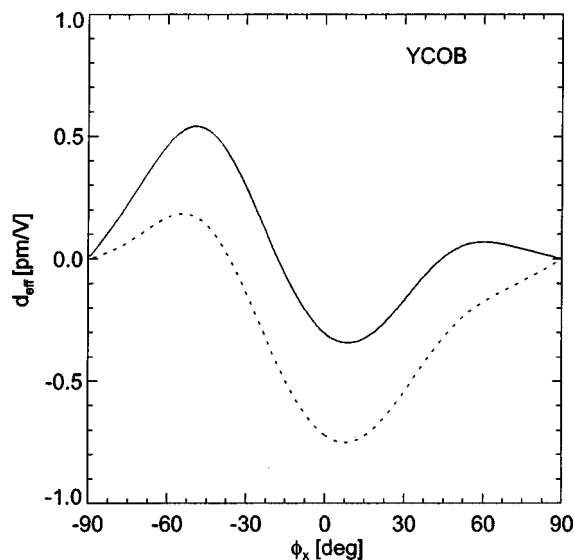


Fig. 7. Calculated values of d_{eff} for type-II frequency doubling of 1320-nm light in YCOB. The solid curve is calculated with our d tensor, and the dashed curve is $0.73 \times d_{\text{eff}}$ calculated from Wang's tensor.¹⁰

C. Discussion

It is clear from a study of Tables 3 and 4 that there are substantial differences between our results and those of some previous reports. In most cases the previous d tensors were deduced from measurements of d_{eff} along various phase-matching directions. It is possible to derive some of the tensor elements accurately by this method, but deriving the full tensor is a difficult task if only limited data are available, as is the case here in which only type-I doubling of 1064-nm light has been characterized. These limited data are insufficient to derive unique and meaningful values for all the d coefficients. For example, d_{xxx} contributes little to d_{eff} in any of these measurements, so its value cannot be derived with much accuracy. Additionally, the coefficients d_{zzz} and d_{zzx} have nearly identical contributions as a function of the phase-matching angle, making it difficult to separate their individual contributions. Only a weighted sum of the two can be deduced. Thus the d tensors derived by Wang *et al.*¹⁰ may fit the d_{eff} data well but still contain substantial errors.

In Figs. 5 and 6 we compare the values of d_{eff} computed by using our d tensor with those computed using Wang's tensor and with measured values from the literature. Figure 1 shows the phase-matching loci for YCOB. GCOB's curve is similar. As we discussed earlier, we need to specify d_{eff} in two octants, one adjacent to the a axis and one adjacent to the c axis. We display d_{eff} for the two octants with $y > 0$ and specify the location with the azimuthal angle ϕ_x measured about the x axis from the xy plane toward the xz plane. Negative values of ϕ_x lie in the a octant, and positive values lie in the c octant. In both Figs. 5 and 6 the solid curves are d_{eff} calculated with our d tensor, and the dashed curves are computed with Wang's tensor scaled down by the factor 0.73. The square symbols represent Wang's measured d_{eff} 's also scaled down by 0.73; the triangles represent the measured values of Adams without scaling; and the diamond

symbols in Fig. 6 are the measured values of Chen scaled as described above to account for improved KTP nonlinearity values.

It is clear that our d tensor matches the measured values for d_{eff} quite well for both crystals. However, so does Wang's. On the other hand, our tensor predicts quite different results from Wang's for other mixing processes such as type-II doubling of 1320-nm light, as may be seen in Fig. 7. The solid curve is calculated from our tensor, and the dashed curve is calculated from Wang's tensor scaled by 0.73. We do not know of any experimental data to compare with these predictions.

ACKNOWLEDGMENTS

We thank Mark Rodriguez of Sandia National Laboratories for help in interpreting our x-ray diffraction measurements and Binh Do of Sandia National Laboratories for help in locating the optical axes of our crystals. Sandia is a multiprogram laboratory operated by Sandia Corporation, a Lockheed Martin Company, for the U.S. Department of Energy's National Nuclear Security Administration under contract DE-AC04-94AL85000.

A. V. Smith, the corresponding author, may be reached by e-mail at arlsmith@sandia.gov.

REFERENCES

1. L. X. Li, M. Guo, H. D. Jiang, X. B. Hu, Z. S. Shao, J. Y. Wang, J. Q. Wei, H. R. Xia, Y. G. Liu, and M. H. Jiang, "Growth and spectra of YCOB and Nd:YCOB crystals," *Cryst. Res. Technol.* **35**, 1361–1371 (2000).
2. P. Segonds, B. Boulanger, J.-P. Feve, B. Menaert, J. Zaccaro, G. Aka, and D. Pelenc, "Linear and nonlinear optical properties of the monoclinic $\text{Ca}_4\text{YO}(\text{BO}_3)_3$ crystal," *J. Opt. Soc. Am. B* **21**, 765–769 (2004).
3. Z. Shao, J. Lu, Z. Wang, J. Wang, and M. Jiang, "Anisotropic properties of Nd:ReCOB (Re = Y, Gd): a low symmetry self-frequency doubling crystal," *Prog. Cryst. Growth Character. Mater.* **40**, 63–73 (2000).
4. N. Umemura, H. Nakao, H. Furuya, M. Yoshimura, Y. Mori, T. Sasaki, K. Yoshida, and K. Kato, "90° phase-matching properties of $\text{YCa}_4\text{O}(\text{BO}_3)_3$ and $\text{Gd}_x\text{Y}_{1-x}\text{Ca}_4\text{O}(\text{BO}_3)_3$," *Jpn. J. Appl. Phys.* **40**, 596–600 (2001).
5. M. Iwai, T. Kobayashi, H. Furuya, Y. Mori, and T. Sasaki, "Crystal growth and optical characterization of rare-earth (Re) calcium oxyborate $\text{ReCa}_4\text{O}(\text{BO}_3)_3$ (Re = Y or Gd) as new nonlinear optical material," *Jpn. J. Appl. Phys.* **36**, L276–L279 (1997).
6. G. Aka, A. Kahn-Harari, F. Mougél, D. Vivien, F. Salin, P. Coquelin, P. Colin, D. Pelenc, and J. P. Damelet, "Linear and nonlinear-optical properties of a new gadolinium calcium oxyborate crystal, $\text{Ca}_4\text{GdO}(\text{BO}_3)_3$," *J. Opt. Soc. Am. B* **14**, 2238–2247 (1997).
7. G. Aka, F. Mougél, D. Pelenc, B. Ferrand, and D. Vivien, "Comparative evaluation of GdCOB and YCOB nonlinear optical properties in principal and out of principal plane configurations for the 1064 nm Nd:YAG laser frequency conversion," in *Nonlinear Materials, Devices, and Applications*, J. W. Pierce, ed., Proc. SPIE **3928**, 108–114 (2000).
8. J. J. Adams, C. A. Ebberts, K. I. Schaffers, and S. A. Payne, "Nonlinear optical properties of $\text{LaCa}_4\text{O}(\text{BO}_3)_3$," *Opt. Lett.* **26**, 217–219 (2001).
9. F. Mougél, G. Aka, F. Salin, D. Pelenc, B. Ferrand, A. Kahn-Harari, and D. Vivien, "Accurate second harmonic generation phase matching angles prediction and evaluation of

- nonlinear coefficients of $\text{Ca}_4\text{YO}(\text{BO}_3)_3$ (YCOB) crystal," in *Advanced Solid-State Lasers*, M. M. Fejer, H. Injeyan, and U. Keller, eds., Vol. 26 of OSA Trends in Optics and Photonics Series (Optical Society of America, Washington, D.C., 1999), pp. 709–714.
10. Z. Wang, J. Liu, R. Song, H. Jiang, S. Zhang, K. Fu, C. Wang, J. Wang, Y. Liu, J. Wei, H. Chen, and Z. Shao, "Anisotropy of nonlinear-optical property of RCOB (R = Gd,Y) crystal," *Chin. Phys. Lett.* **18**, 385–387 (2001).
 11. C. Chen, Z. Shao, J. Jiang, J. Wei, J. Lin, J. Wang, N. Ye, J. Lv, B. Wu, M. Jiang, M. Yoshimura, Y. Mori, and T. Sasaki, "Determination of the nonlinear optical coefficients of $\text{YCa}_4\text{O}(\text{BO}_3)_3$ crystal," *J. Opt. Soc. Am. B* **17**, 566–571 (2000).
 12. C. Chen, N. Ye, J. Lin, J. Jiang, W. Zeng, and B. Wu, "Computer-assisted search for nonlinear optical crystals," *Adv. Mater.* **11**, 1071–1078 (1999).
 13. N. Umemura, M. Ando, K. Suzuki, E. Takaoka, K. Kato, M. Yoshimura, Y. Mori, and T. Sasaki, "Temperature-insensitive second-harmonic generation at $0.5321\ \mu\text{m}$ in $\text{YCa}_4\text{O}(\text{BO}_3)_3$," *Jpn. J. Appl. Phys.* **42**, 5040–5042 (2003).
 14. R. J. Gehr and A. V. Smith, "Separated-beam nonphase-matched second-harmonic method of characterizing nonlinear optical crystals," *J. Opt. Soc. Am. B* **15**, 2298–2307 (1998).
 15. M. V. Pack, D. J. Armstrong, and A. V. Smith, "Measurement of the $\chi^{(2)}$ tensor of the potassium niobate crystal," *J. Opt. Soc. Am. B* **20**, 2109–2116 (2003).
 16. D. J. Armstrong, M. V. Pack, and A. V. Smith, "Instrument and method for measuring second-order nonlinear optical tensors," *Rev. Sci. Instrum.* **74**, 3250–3257 (2003).
 17. D. Klimm, S. Ganschow, R. Bertram, J. Doeschel, V. Bermudez, and A. Klos, "Phase separation during the melting of oxide borates $\text{LnCa}_4\text{O}(\text{BO}_3)_3$ (Ln = Y, Gd)," *Mater. Res. Bull.* **37**, 1737–1747 (2002).
 18. D. A. Roberts, "Simplified characterization of uniaxial and biaxial nonlinear optical crystals: a plea for standardization of nomenclature and conventions," *IEEE J. Quantum Electron.* **28**, 2057–2074 (1992).
 19. G. D. Boyd and D. A. Kleinman, "Parametric interaction of focused Gaussian light beams," *J. Appl. Phys.* **39**, 3597–3639 (1968).
 20. M. V. Pack, D. J. Armstrong, and A. V. Smith, "Measurement of the $\chi^{(2)}$ tensors of KTiOPO_4 , KTiOAsO_4 , RbTiOPO_4 , and RbTiOAsO_4 crystals," *Appl. Opt.* **43**, 3319–3323 (2004).